Chemical Physics 457 (2015) 63–69

Contents lists available at ScienceDirect

Chemical Physics

journal homepage: www.elsevier.com/locate/chemphys

Determination of contact angle of droplet on convex and concave spherical surfaces

Dongyin Wu [a,1], Pengfei Wang [b,c,1], Ping Wu [a,c], Qingzhen Yang [c,d], Fusheng Liu [c,d], Yulong Han [c,d], Feng Xu [c,d], Lin Wang [c,d,*]

[a] School of Energy and Power Engineering, Xi'an Jiaotong University, Xi'an 710049, China
[b] Qian Xuesen Laboratory of Space Technology, China Academy of Space Technology, Beijing 100094, China
[c] Bioinspired Engineering and Biomechanics Center, Xi'an Jiaotong University, Xi'an 710049, China
[d] The Key Laboratory of Biomedical Information Engineering of Ministry of Education, School of Life Science and Technology, Xi'an Jiaotong University, Xi'an 710049, China

ARTICLE INFO

Article history:
Received 20 March 2015
In final form 18 May 2015
Available online 1 June 2015

Keywords:
Contact angle
Wetting
Curved surfaces
Modeling

ABSTRACT

Experimentally measuring the apparent contact angle on a curved surface usually requires a specific instrument, which could be costly and is not widely accessible. To address this challenge, we proposed a simple wetting model to theoretically predict the apparent contact angle of a droplet on convex and concave spherical surfaces, which requires knowing the volume of the droplet, surface curvature and intrinsic contact angle. Using this theoretical model, we investigated the influence of radius and hydrophobicity of curved surfaces on wetting behaviors. For a concave surface, the droplet on it could exhibit a convex or concave morphology depending on the detailed parameters. The critical volume for a droplet changing from convex to concave shape was determined in this study. Employing this model, the contact angle on curved surface with microstructures was also investigated. The model may contribute to the understanding of natural wetting phenomenon and better design of related structures.

1. Introduction

The contact angle of a droplet on a curved surface is widely involved in the fields of engineering [1,2], biomedicine [3], and natural world [4,5]. For example, curved microstructures fabricated on a surface can modify the hydrophobicity of the surface through affecting droplet-surface interactions [6,7]; changes of droplet shape can be used to characterize the sensitivity and specificity of biomembranes [8]; and some plant leaves and insect wings are capable of high water repellence (e.g., lotus leaf, morpho butterfly) [9–11]. Investigation of droplet contact angle not only contributes to assessing the wettability of the surface (i.e., hydrophilic or hydrophobic ability) and understanding the related natural phenomena, but also promotes the better design of functional surfaces and improves the intellectualization of related structures. For instance, novel artificial materials with super water- or oil-proof capability have been designed through designing special curved surfaces [12,13].

With the contact surface assumed absolutely smooth, stiff, homogenous and inert (i.e., an ideal surface), the relation between contact angle and interfacial tension of a droplet was firstly described by Young's equation [14,15]. Further, whilst the Wenzel equation determined the contact angles on a rough surface for homogeneous wetting regime [16], the Cassie–Baxter equation developed the theories for heterogeneous wetting regime (e.g., porous contact surface) [17]. However, these studies mostly focused on the contact angle of a droplet on flat surface, Fig. 1(a). Recently, a theory of wetting on ideal spherical surfaces, proposed by Extrand and Moon [18] demonstrated that the wetting equation $\theta = \theta(\theta_0, a, R)$ could determine the apparent contact angle θ by experimentally measuring the contact radius a and the intrinsic contact angle θ_0, R being radius of the solid spherical surface, Fig. 1(b). In addition, θ could be quantified through another proposed equation $\theta = \theta(\theta_0, r, R)$, where the droplet radius r is experimentally measured [19]. Besides spherical surfaces, a recent study extended the theory to concave surfaces and proposed a different wetting equation $\theta = \theta(V_L, a, R)$, where the droplet volume (V_L) could be manually controlled in the experiment [20], Fig. 1(c). However, it is technically challenging to measure the horizontal contact area between the droplet and nonplanar surface, the center of the hemispherical droplet, and the intrinsic contact angle on nonplanar surface, which has limited the practical applications of these theories on convex and concave spherical surfaces. Therefore, there is still an unmet need for a wetting model that

* Corresponding author at: Bioinspired Engineering and Biomechanics Center, Xi'an Jiaotong University, Xi'an 710049, China.
E-mail address: wanglin0527@126.com (L. Wang).
[1] Authors contributed equally to this work.

http://dx.doi.org/10.1016/j.chemphys.2015.05.020
0301-0104/

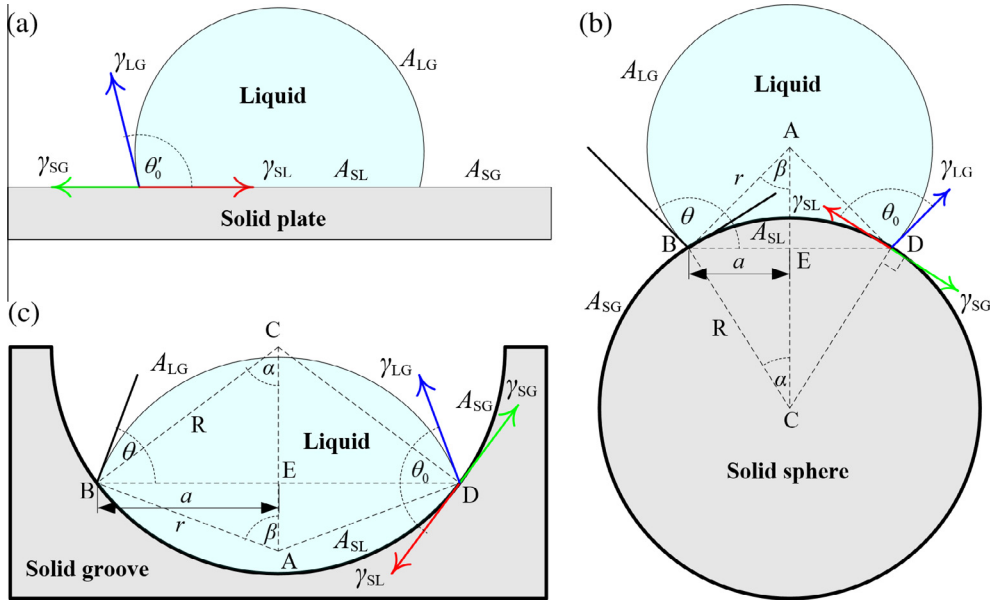

Fig. 1. Schematic of a droplet on different surfaces. (a) Flat surface. (b) Convex surface. (c) Concave surface. A_{LG}, A_{SL} and A_{SG} are separately areas of liquid–air, liquid–solid and solid–air interfaces; γ_{LG}, γ_{SL} and γ_{SG} are related coefficients of surface tension.

can be readily employed to determine the contact angle of a droplet on convex and concave spherical surfaces.

Measuring the apparent contact angles on the curved surfaces could be expensive, and usually the specific instruments are necessary. In this study, we proposed a simple wetting model to predict the apparent contact angle on curved surfaces $\theta = \theta(\theta_0', V_L, R)$, which describes the quantitative relation between the apparent contact angle θ and the intrinsic contact angle on flat surface θ_0', the curvature R and the droplet volume V_L. For the intrinsic contact angle, θ_0', it is a known constant parameter for the droplet and the ideal curved surface made of known materials. For most material, θ_0' is already available in handbooks. The curvature of the convex or concave (i.e., R) is measured with ease, and the droplet volume V_L is known as the liquid could be controlled when dripping it. Thus, it avoids the need for the specific equipment. This theoretical model was verified by performing a set of experiments on contact angles of droplets on spherical and concave surfaces. Then it was employed to investigate the influence of different parameters on the apparent contact angles. In addition, this model was extended to discuss the contact angle on curved surfaces with microstructures.

As for the applicability, predicting the apparent contact angle and thus the morphology of the droplet on curved surface could be significantly important. Wetting behavior on ideally flat surfaces merely occurs in lab experiments. However, curved surfaces are more widely encountered in nature and industrial process. For instance, cactus' spines could collect fog from the air due to the wetting behavior on curved surfaces [25]. This is much favorable for the cactus to survive in the desert. Some research has shown that the wetting behavior on curved surface can be used to separate oil from water [26], which is significant as we are now facing a more and more critical energy crisis. Thus studying the wetting behavior on curved surfaces could help understanding the nature and may have potential applications in engineering.

2. Theoretical model

When a drop spreads on an ideal solid surface (Fig. 1), the contact area between the liquid and the solid surface (i.e., liquid–solid interface), A_{SL}, becomes larger. Meanwhile, the contact area between the solid surface and air (i.e., solid–air interface), A_{SG}, decreases, as $A_{SG} + A_{SL} =$ constant. However, dependent upon the apparent contact angle θ, the changing trend of the contact area between the liquid and air (i.e., liquid–air interface), A_{LG}, varies. According to Young's theory on interface energy and with the effects of gravity ignored [21], thermodynamic equilibrium of the system dictates:

$$\frac{dA_{LG}}{dA_{SL}} = \frac{\gamma_{SG} - \gamma_{SL}}{\gamma_{LG}} \tag{1}$$

where γ_{SG}, γ_{SL} and γ_{LG} are separately the coefficients of surface tension amongst the three objects. Depending only on the materials, temperature and pressure, these parameters remain constant in experiments. Eq. (1) is valid for flat, spherical and concave surfaces. For a flat surface, Eq. (1) reduces to Young's equation: $dA_{LG}/dA_{SL} = \cos\theta_0'$. For a spherical surface, by considering small changes $d\beta$ and $d\alpha$, the area of liquid–air interface is determined by the integral equation $A_{LG} = \int_\beta^\pi 2\pi r^2 \sin\beta d\beta$ while the area of liquid–solid interface is calculated by $A_{SL} = \int_0^\alpha 2\pi R^2 \sin\alpha d\alpha$. Based on the assumption of liquid incompressibility and the geometrical relations among the angles of curvatures (α, β), radius of droplet (r) and contact angles (θ, θ_0), we arrived at (see Appendix):

$$\frac{dA_{LG}}{dA_{SL}} = \cos\theta_0 \tag{2}$$

It has been demonstrated that Eq. (2) also holds true for a concave surface. Because γ_{SG}, γ_{SL} and γ_{LG} are constant for given materials and environment, regardless of the shape of the contact surface, Eqs. (1) and (2) suggest that the intrinsic contact angle on an ideal curved surface equals the one on an ideal flat surface, i.e., $\theta_0 = \theta_0'$, which are both constant. In other words, θ_0 could be determined by measuring the contact angle of a droplet on a flat surface.

By systematically analyzing the geometrical variables shown in Fig. 1(b) and (c) and adopting the relation between θ_0 and θ_0', we obtained the dimensionless wetting equation for convex and concave spherical surfaces as:

$$V^* = \frac{\sin^3\theta^*}{\sin^3\theta} f(\theta) + n \cdot f(\theta^*) \tag{3}$$

where $f(x) = (2 - 3\cos x + \cos^3 x)/4$ and $V^* = V_L/\left(\frac{4}{3}\pi R^3\right)$. For spherical surfaces, $\theta^* = \theta - \theta_0'$, $n = -1$; for concave surfaces, $\theta^* = \theta_0' - \theta$, $n = 1$. Finally, the contact angle of a droplet on a convex and concave spherical surface could be determined by Eq. (3), i.e., $\theta = \theta(\theta_0', V_L, R)$.

The aforementioned relation $\theta = \theta(\theta_0', V_L, R)$ can find its applications in predicting the apparent contact angles on curved surfaces. The main merits of this method lies in two aspects. Firstly, this relation is straightforward and all dependent variables could be obtained with ease. As stated before, the intrinsic contact angle θ_0' can be looked up in handbooks. Liquid volume V_L is usually known when dropping it onto the curved surface. Curvature R can also be measured easily. Secondly, for a concave surface, the apparent contact angle is impossible to be experimentally measured as the liquid–solid interface is always blocked by the solid or the droplet. The theoretical model in this study provides a means to predict the apparent contact angle on a concave surface.

To formulate the proposed wetting model, it was assumed that the gravity of droplet is negligible and hence the liquid–air interface is taken as spherical; due to gravity effect, the shape of a droplet changes from spherical to nonspherical with increasing droplet volume [22]. Consequently, the critical volume of the phase transition is important to determine the applicable range of the present theoretical model, as analyzed below.When the droplet is small and exhibits a spherical shape, the height between its top and the horizontal line passing through the liquid–air–solid crossover points is:

$$h = a\tan\frac{\theta}{2} \tag{4}$$

When the droplet is large and exhibits a non-spherical shape due to gravity effect, the height between its top and the horizontal line becomes [23]:

$$h' = \left[2\left(\frac{\gamma_{LG}}{\rho g}\right)(1-\cos\theta)\right]^{1/2}\left[1 + \left(\frac{\gamma_{LG}}{\rho g}\right)^{1/2}\frac{2}{2a}\right]^{-1/2} \tag{5}$$

where ρ is the density of the liquid and g is the coefficient of gravitational acceleration.

When the droplet shape transforms from sphericity to non-sphericity, $h = h'$ holds. Given that the contact radius a equals $R\sin(\theta - \theta_0)$ for spherical surfaces and $R\sin(\theta_0 - \theta)$ for concave surfaces, the apparent contact angle θ at transition can be obtained by solving Eqs. (4) and (5). Subsequently, upon substituting θ into (3), the critical volume of the droplet is determined. For concave surfaces, however, solving (4) and (5) cannot always give a reasonable value of θ, affected by the radius (R) of the convex and concave spherical surface. This implies that the liquid–air interface remains spherical and does not become non-spherical until the convex and concave spherical interface extends into a flat one with increasing droplet volume, i.e., it always has that $h \neq h'$. Under such conditions, the critical volume of the droplet exists when the liquid–air interface becomes flat (i.e., $\theta = 0$), which could be determined by reducing Eq. (3) to $V_L = \frac{4\pi}{3}R^3 f(\theta_0)$. In addition, the critical value of R corresponding to the inequality between h and h' could be calculated via extreme value analysis of equation $h = h'$.

3. Experiments

Experimentally, to determine the contact angle of a droplet on convex and concave spherical surfaces, we used ultrapure water (coefficient of surface tension $\gamma = 72$ mN/m and density $\rho = 998$ kg/m^3) as droplet medium. Polytetrafluoroethylene (PTFE, $\theta_0' = 108^\circ$) and polycarbonate (PC, $\theta_0' = 89^\circ$), supplied by McMaster Car LLC (US) and having perfect properties of chemical inertness, smoothness and homogeneity, were selected to construct solid surfaces. For the measurement of contact angles, a commercial instrument (model: POWEREACH JC2000CA) with accuracy of 0.1° was employed, and the minimum droplet volume produced by the liquid injector was 0.1 μL. With critical dropt volume considered, in the experiments we orderly chose 3 μL, 5 μL, 7 μL, 9 μL and 11 μL as the droplet volume, and 6.4, 12.7 mm as the diameter of solid spherical surfaces. The experiments were only performed on spherical surfaces due to limitation on measuring contact angle of droplets on concaved surfaces, as the liquid–solid interface was always covered by the upper droplet. As a result, in the present study, we first used a series of experimental data on spherical surfaces to validate the proposed wetting model and then theoretically predicted important characteristics of droplets on spherical and concaved surfaces.

4. Results and discussion

4.1. Apparent contact angle on convex and concave spherical surfaces

To verify the constancy of apparent contact angles θ_0', we repeatedly measured θ_0' of water droplets on flat PTFE and PC surfaces. The results demonstrated that θ_0' were $108.0 \pm 0.44^\circ$ and $89.0 \pm 0.25^\circ$, respectively, which are consistent with existing reports [20]. Consequently, we set $\theta_0' = 108^\circ$ for water on PTFE and $\theta_0' = 89^\circ$ for PC.

Theoretical and experimental determinations of droplet contact angles on PTFE spherical surfaces were both presented in Fig. 2(a). Excellent agreement between theory and experiment is observed. As the droplet volume (V_L) is increased, the liquid–solid interface becomes larger and the apparent contact angle θ increases. With droplet volume fixed, θ for a spherical surface of diameter $2R = 6.4$ mm is considerably bigger than that with diameter $2R = 12.7$ mm. This implies that a smaller apparent contact angle is induced if the radius of the solid surface is larger and approaches the principle contact angles if R is sufficiently large, i.e., $\theta \to 108^\circ$. Similar results for droplets on PC surfaces were shown in Fig. 2(b). Again, the theory agreed well with experiment. For droplets with same volume, the apparent contact angle for PC surfaces is smaller than that for PTFE surfaces. Further, θ increases with increasing V_L but decreases with increasing R. In addition to our experiments of water droplets on PTFE and PC spherical surfaces, existing experimental results of Ethylene Glycol (EG) droplets on PTFE surfaces 18 were compared in Fig. 2(c) with our model predictions (for EG droplets on PTFE surfaces, θ_0' = 89°). For the case of $2R = 6.4$ mm, the small deviation of theory from experiment may be attributed to surface roughness, experiment operation, etc.

4.2. Contact area on convex and concave spherical surfaces

The area of liquid–solid interface depends not only on droplet volume but also on surface hydrophobicity. For a given solid spherical or concave surface, the angle of curvature α may be adopted to characterize changes in contact area whereas the principle contact angle θ_0' reflects surface hydrophobicity (e.g., the surface becomes more hydrophobic with increasing θ_0'). Fig. 3(a) plotted α of spherical surfaces ($R = 6.4$ mm) as a function of V_L for selected values of θ_0'. With increasing droplet volume, the angle of curvature slowly increases. However, it decreases as θ_0' becomes larger. These results indicate that the contact area shrinks if the surface is more hydrophobic and extends if the droplet volume increases. Similar

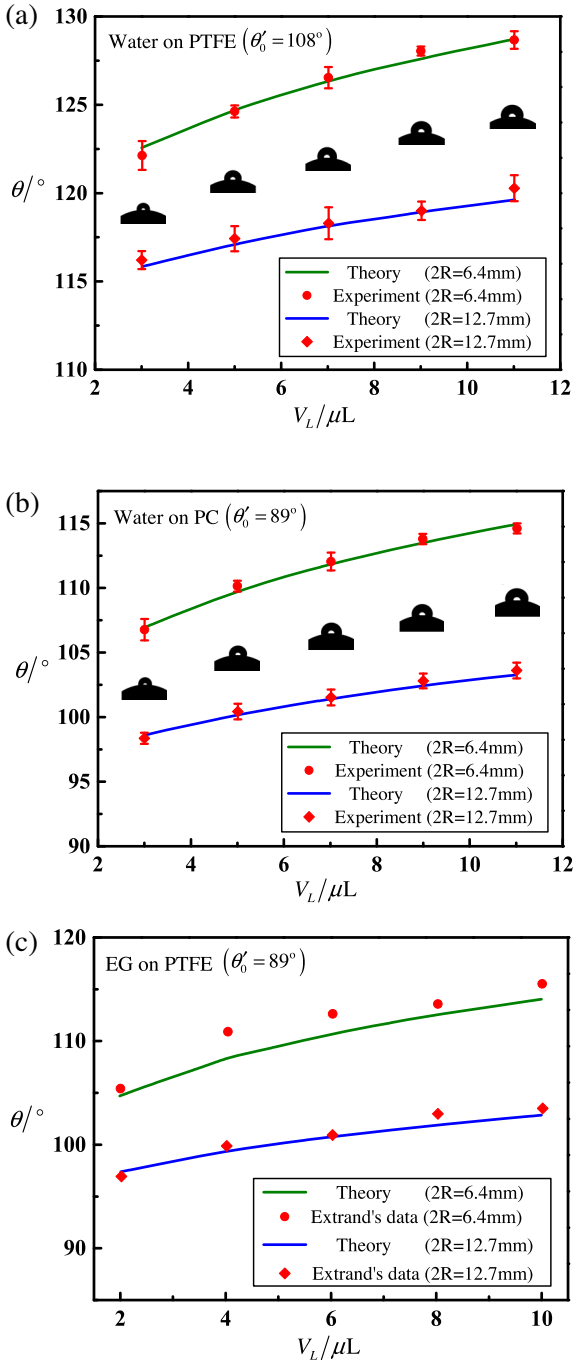

Fig. 2. Theoretical prediction and experimental measurement of apparent contact angle of liquid droplet on curved surfaces. (a) Water droplet on PTFE surface. (b) Water droplet on PC surface. (c) EG droplet on PTFE surface.

behaviors were observed for droplets on concave surfaces, as shown in Fig. 3(b). There is nonetheless a breakpoint for the curve of $\theta_0' = 30^\circ$, representing the maximum droplet volume for spherical liquid–air interfaces. If V_L is smaller than this critical value, the droplet may be taken as a sphere. If V_L exceeds this critical value, the behavior cannot be predicted by the present theory as the effect of gravity was neglected.

4.3. Critical volume of droplet on concave surface

As stated before, the droplet on a concave surface could exhibit a convex or concave shape depending on the detailed parameters,

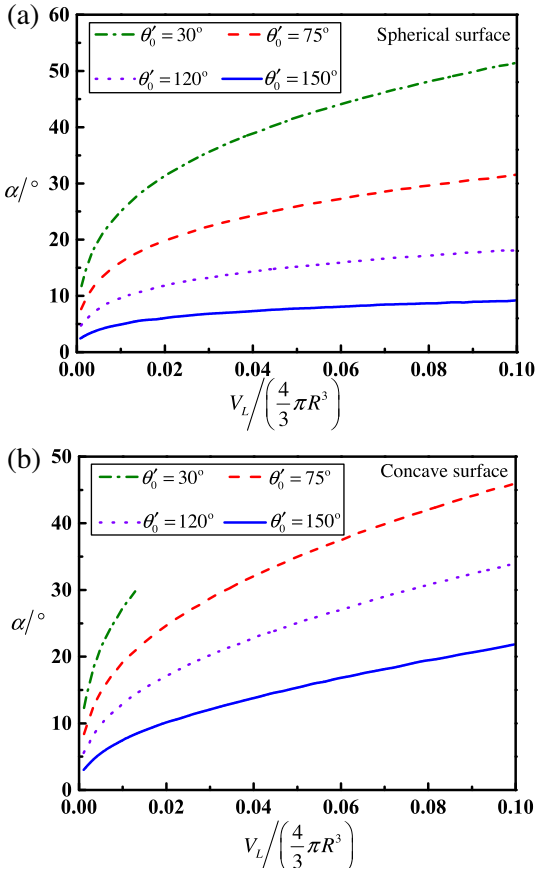

Fig. 3. Angle of liquid–solid curvature of droplet on convex and concave spherical surfaces plotted as a function of droplet volume for selected principle contact angles. (a) Droplet on a convex surface. (b) Droplet on a concave surface.

such as the intrinsic contact angle, droplet volume and radius of solid surface (see the inset of Fig. 4). Another factor that influences the droplet morphology is the gravitational force. With the increase of the gravity, the droplet tends to be flatten at its top and thus being no longer a spherical shape. These two cases, the droplet transfers from a convex to concave shape, and the droplet changes from spherical to non-spherical due to gravity, are referred as the phase transition. To further analyze the phase

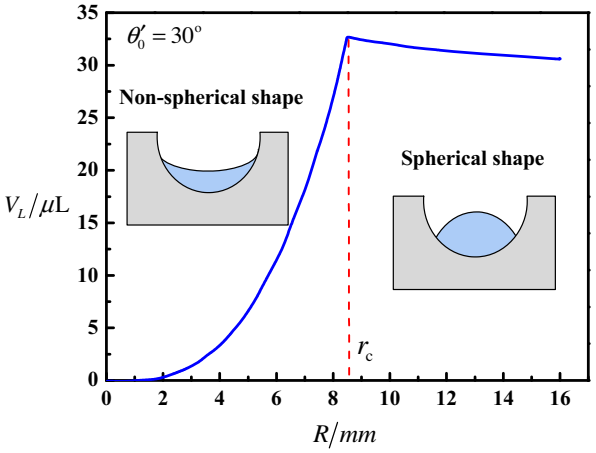

Fig. 4. Phase transition of droplet shape on a concave surface with respect to surface radius and droplet volume. r_C is the critical surface radius for phase transition between a convex liquid–air interface and a concave liquid–air interface.

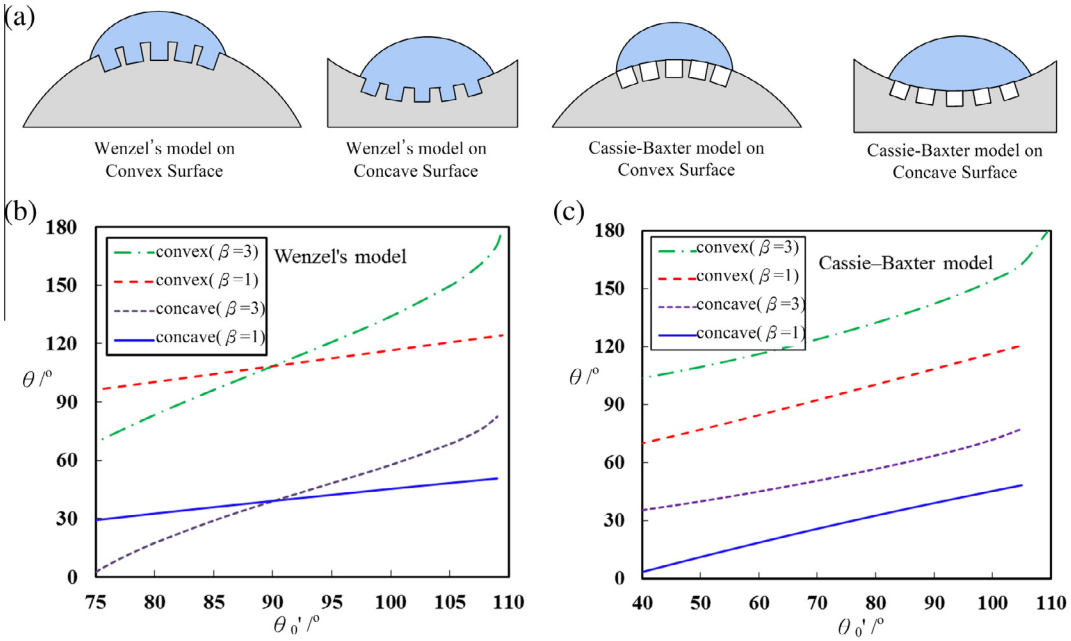

Fig. 5. Apparent contact angle on convex and concave spherical surfaces with microstructures. The volume of the droplet is $V^* = V_L/\left(\frac{4}{3}\pi R^3\right) = 0.025$. (a) Schematic of droplet's wetting behavior on curved surfaces with microstructures. (b) The apparent contact angle under Wenzel's model (i.e., completely wetting). (c) The apparent contact angle under Cassie–Baxter model (i.e., partially wetting).

transition of droplet shape, we fix the intrinsic contact angle $\theta_0' = 30^\circ$ and investigate the critical volume with respect to the radius R of solid concave surface, Fig. 4. Let r_c represents the critical value of R that induces the inequality between h and h'. When $R < r_c$ the transition of shape from convex to concave occurs before the transition from spherical to non-spherical. The liquid–air interface remains spherical until this interface becomes flat with the increase of liquid volume. The critical volume which corresponds the shape from a convex to concave is then calculated by Eq. (3) with $\theta = 0^\circ$. On the other hand, when $R > r_c$, the transition from spherical to non-spherical due to gravitational force occurs first. The critical volume is determined by solving Eq. (3) and $h = h'$. If the droplet volume is smaller than the critical volume, the gravity effect of droplet could be neglected and the shape of liquid–air surface is spherical.

4.4. Apparent contact angle on pre-structured convex and concave spherical surfaces

This theory could be modified with ease to study the wetting behavior on convex and concave spherical surfaces with microstructures. For flat surfaces, it is well know that there are two models to describe the contact angle on rough surface (i.e., the surface with microstructures), the Wenzel's model and the Cassie–Baxter model. If the liquid can wet the rough surface completely (see Fig. 5(a)), the apparent contact angle is governed by the Wenzel's equation [24]. For a convex or concave spherical surface with microstructures, the apparent contact angle can be obtained by a straightforward combination of the Wenzel's equation and Eq. (3).

$$\begin{cases} \cos\theta_0' = \beta\cos\theta_0 \\ V^* = \frac{\sin^3\theta^*}{\sin^3\theta} f(\theta) + n\cdot f(\theta^*) \end{cases} \tag{6}$$

where β is the roughness ratio, $f(x) = (2 - 3\cos x + \cos^3 x)/4$ and $V^* = V_L/\left(\frac{4}{3}\pi R^3\right)$ as stated before. For spherical convex surfaces, $\theta^* = \theta - \theta_0'$, $n = -1$; for concave surfaces, $\theta^* = \theta_0' - \theta$, $n = 1$.

Employing Eq. (6), the apparent contact angles can be obtained, which are depicted in Fig. 5(b). The volume of droplet is specified as $V^* = V_L/\left(\frac{4}{3}\pi R^3\right) = 0.025$ and, both convex and concave surfaces are investigated. As can be seen, the apparent contact angles increase with intrinsic contact angles and, the values are also closely dependent on the roughness ratio β. However, there is a particular point on the curve, for a specific curved surfaces, the apparent contact angle is independent on the roughness if the intrinsic contact angle equals 90°.

Another wetting theory for the contact angle on rough surface would be Cassie–Baxter model, which is suitable for the case that the liquid partially wets the rough surface [24]. If a curved surface is rough, then the apparent contact angle can be described by the combination of Cassie–Baxter equation and Eq. (3), which express as follows,

$$\begin{cases} \cos\ \theta_0' = \beta\eta\cos\theta_0 + \eta - 1 \\ V^* = \frac{\sin^3\theta^*}{\sin^3\theta} f(\theta) + n\cdot f(\theta^*) \end{cases} \tag{7}$$

where the β is the roughness ratio of the wet surface area and η is the fraction of solid surface area wet by the liquid. The $f(x)$, V^*, θ^* and n are the same as explained before. For simplification, $\eta = 1/\beta$, indicating that the liquid only wets the top surface of the structures as shown in Fig. 5(a). The apparent contact angles obtained by Eq. (7) are depicted in Fig. 5(c). Comparing the curves of $\beta = 3$ and that of $\beta = 1$ ($\beta = 1$ represents an ideal smooth surface), one can see that the apparent contact angles would increase significantly by the microstructures on the surfaces.

5. Conclusions

We developed a simple wetting model to determine the apparent contact angle of a droplet on spherical and concave surfaces, which can be calculated if the volume of the droplet is known. The model predictions agreed well with experimental measurements of water droplets on PTFE and PF surfaces and existing data of EG droplets on PTFE surfaces. The influence of droplet volume

and surface hydrophobicity on the apparent contact angle as well as area of liquid–solid interface was quantified. For droplets on concave surfaces, the critical droplet volume corresponding to the phase transition of liquid–air interfaces was determined. This model was then employed to investigate the apparent contact angle on rough curved surfaces.

Conflict of interest

There is no conflict of interest.

Acknowledgments

This work was financially supported by the National Natural Science Foundation of China (11372243), the International Science & Technology Cooperation Program of China (2013DFG02930), the Key Program for International S&T Cooperation Projects of Shaanxi (2014KW12-01), China Postdoctoral Science Foundation (2013M532054) and "Zhi Gu" Innovation Program of Southern China.

Appendix A. Calculating dA_{LV}/dA_{SL} with the constrain of constant volume

A.1. Convex case

Consider the drop whose cross section is drawn in Fig. 1b. As it is purely geometrical, we denote A_{LV} as A_r so as to remember that this is the cap surface of a sphere of radius r, and A_{SL} as A_R so as to remember that this is the cap surface of the solid sphere of radius R.

To determine the exact angle, θ, we need to know what is the size of sphere of radius r that the drop is taken from. The volume of the drop, V, is a volume of the spherical cap of radius r (V_{r-C}) minus the volume of the spherical cap of radius R (V_{R-C}).

First we calculate V_{r-C} and V_{R-C}

$$V_{r-C}=\int_0^{\theta}\pi r^3\sin^3\beta d\beta=\frac{4\pi}{3}r^3\left(\frac{2-3\cos\theta+\cos^3\theta}{4}\right) \tag{A.1}$$

$$V_{R-C}=\int_0^{\alpha}\pi R^3\sin^3\alpha d\alpha=\frac{4\pi}{3}R^3\left(\frac{2-3\cos\alpha+\cos^3\alpha}{4}\right) \tag{A.2}$$

Here we assume a dimensionless function, which means the ratio of spherical cap volume to the sphere volume with an identical radius.

$$f(x)=\frac{2-3\cos x+\cos^3 x}{4} \tag{A.3}$$

Hence the volume, V, of the drop that we are interested in is

$$V=V_{r-C}-V_{R-C}=\frac{4\pi}{3}[r^3f(\theta)-R^3f(\alpha)] \tag{A.4}$$

We can use the geometrical relations

$$\frac{R}{r}=\frac{\sin\beta}{\sin\alpha},\quad \theta+\beta=\pi,\quad \theta-\theta_0=\alpha$$

and rewrite Eq. (A.4) as

$$V=\frac{4\pi}{3}r^3\left[f(\theta)-\frac{\sin^3\theta}{\sin^3(\theta-\theta_0)}f(\theta-\theta_0)\right] \tag{A.5}$$

$$V=\frac{4\pi}{3}R^3\left[\frac{\sin^3(\theta-\theta_0)}{\sin^3\theta}f(\theta)-f(\theta-\theta_0)\right] \tag{A.6}$$

Hence the radius, r, can be expressed in terms of the volume, V, and the angle θ

$$r=\left(\frac{3V}{4\pi}\right)^{1/3}\left[f(\theta)-\frac{\sin^3\theta}{\sin^3(\theta-\theta_0)}f(\theta-\theta_0)\right]^{-1/3} \tag{A.7}$$

Second we need to find expressions for A_r and A_R

$$A_r=\int_{\beta}^{\pi}2\pi r^2\sin\beta d\beta=2\pi r^2(1+\cos\beta)=2\pi r^2(1-\cos\theta) \tag{A.8}$$

$$A_R=\int_0^{\alpha}2\pi R^2\sin\alpha d\alpha=2\pi R^2(1-\cos(\theta-\theta_0)) \tag{A.9}$$

Putting Eq. (A.7) into Eq. (A.8) we get

$$A_r=2\pi(V)^{2/3}\left[\frac{4\pi}{3}f(\theta)-\frac{4\pi\sin^3\theta}{3\sin^3(\theta-\theta_0)}f(\theta-\theta_0)\right]^{-2/3}(1-\cos\theta) \tag{A.10}$$

Now that we have both A_r and A_R expressed in terms of constant volume and intrinsic contact angle as a function of only the angle of contact, θ, we can use the chain rule to find dA_r/dA_R

$$\frac{dA_r}{dA_R}=\left(\frac{dA_r}{d\theta}\right)\Big/\left(\frac{dA_R}{d\theta}\right)$$

After performing both derivatives, dividing them and rearranging we get

$$dA_r/dA_R=\cos\theta_0. \tag{A.11}$$

A.2. Concave case

Consider a sessile liquid drop of volume V in a spherical cavity of a solid (Fig. 1c). The analysis of the concave case differs from that of the convex case in two aspects. First, the intrinsic contact angle (θ_0) is the sum of the apparent value (θ) and the curvature angle (α)

$$\theta+\alpha=\theta_0$$

Second, the liquid drop volume (V) is the sum of apparent spherical cap volume (V_{r-C}) and the inverse spherical cap volume (V_{R-C})

$$V=V_{r-C}+V_{R-C} \tag{A.12}$$

By following the approach given above, we can get

$$V=\frac{4\pi}{3}r^3\left[f(\theta)+\frac{\sin^3\theta}{\sin^3(\theta_0-\theta)}f(\theta_0-\theta)\right] \tag{A.13}$$

$$V=\frac{\pi}{3}R^3\left[\frac{\sin^3(\theta_0-\theta)}{\sin^3\theta}f(\theta)+f(\theta_0-\theta)\right] \tag{A.14}$$

We write for the radius r, A_r and A_R

$$r=\left(\frac{3V}{4\pi}\right)^{1/3}\left[f(\theta)+\frac{\sin^3\theta}{\sin^3(\theta_0-\theta)}f(\theta_0-\theta)\right]^{-1/3} \tag{A.15}$$

$$A_r=2\pi r^2(1-\cos\theta)=2\pi(V)^{2/3}\left[\frac{4\pi}{3}f(\theta)+\frac{4\pi\sin^3\theta}{3\sin^3(\theta_0-\theta)}f(\theta_0-\theta)\right]^{-2/3}(1-\cos\theta) \tag{A.16}$$

$$A_R=\int_0^{\alpha}2\pi R^2\sin\alpha d\alpha=2\pi R^2[1-\cos(\theta_0-\theta)] \tag{A.17}$$

Repeating the process above, we finally obtain

$$dA_r/dA_R=\cos\theta_0. \tag{A.18}$$

References

[1] N.A. Malvadkar, M.J. Hancock, K. Sekeroglu, W.J. Dressick, M.C. Demirel, Nat. Mater. 9 (2010) 1023.
[2] J.C. Bird, R. Dhiman, H.M. Kwon, K.K. Varanasi, Nature 503 (2013) 385.
[3] B. Bhushan, Y.C. Jung, Prog. Mater. Sci. 56 (2011) 1.

[4] Y. Zheng, H. Bai, Z. Huang, X. Tian, F.Q. Nie, Y. Zhao, J. Zhai, L. Jiang, Nature 463 (2010) 640.
[5] K. Xu, J.R. Heath, Nat. Mater. 12 (2013) 872.
[6] K.H. Chu, R. Xiao, E.N. Wang, Nat. Mater. 9 (2010) 413.
[7] A. Cannon, W. King, J. Micromech. Microeng. 20 (2010) 025018.
[8] Y. Chen, A.W. Gani, S.K. Tang, Lab Chip 12 (2012) 5093.
[9] B. Verberck, Nat. Phys. 10 (2014) 95.
[10] R.A. Potyrailo, H. Ghiradella, A. Vertiatchikh, K. Dovidenko, J.R. Cournoyer, E. Olson, Nat. Photonics 1 (2007) 123.
[11] M.K. Kwak, C. Pang, H.E. Jeong, H.N. Kim, H. Yoon, H.S. Jung, K.Y. Suh, Adv. Funct. Mater. 21 (2011) 3606.
[12] D. Wu, S.Z. Wu, Q.D. Chen, Y.L. Zhang, J. Yao, X. Yao, L.G. Niu, J.N. Wang, L. Jiang, H.B. Sun, Adv. Mater. 23 (2011) 545.
[13] C.T. Hsieh, W.-Y. Chen, Carbon 48 (2010) 612.
[14] X.S. Wang, S.W. Cui, L. Zhou, S.H. Xu, Z.W. Sun, R.Z. Zhu, J. Adhes. Sci. Technol. 28 (2014) 161.
[15] T. Young, Philos. Trans. R. Soc. 95 (1805) 65.
[16] R.J. Good, J. Am. Chem. Soc. 74 (1952) 5041.
[17] A. Giacomello, M. Chinappi, S. Meloni, C.M. Casciola, Phys. Rev. Lett. 109 (2012) 226102.
[18] C. Extrand, S.I. Moon, Langmuir 24 (2008) 9470.
[19] G. Viswanadam, G.G. Chase, J. Colloid Interface Sci. 367 (2012) 472.
[20] C. Extrand, S.I. Moon, Langmuir 28 (2012) 7775.
[21] R. Tadmor, Langmuir 20 (2004) 7659.
[22] M. Guilizzoni, J. Colloid Interface Sci. 364 (2011) 230.
[23] C. Extrand, S.I. Moon, Langmuir 26 (2010) 11815.
[24] A. Marmur, Langmuir 19 (2003) 8343.
[25] J. Ju, H. Bai, Y. Zheng, T. Zhao, R. Fang, L. Jiang, Nat. Commun. 3 (2013) 1247.
[26] K. Li, J. Ju, Z. Xue, J. Ma, L. Feng, S. Gao, L. Jiang, Structured cone arrays for continuous and effective collection of micron-sized oil droplets from water 4 (2013) 2276.